Published in final edited form as:
Hepatology. 2015 February ; 61(2): 497–505. doi:10.1002/hep.27437.

Shp/Npas2 Axis in Regulating the Oscillation of Liver Lipid Metabolism

Sang Min Lee[1,6], **Yuxia Zhang**[2,6], **Hiroyuki Tsuchiya**[2,6], **Rana Smalling**[2], **Anton M. Jetten**[3], and **Li Wang**[1,4,5,*]

[1]Department of Physiology and Neurobiology, University of Connecticut, Storrs, CT 06269

[2]Department of Medicine, University of Utah School of Medicine, Salt Lake City, UT 84132

[3]Cell Biology Section, Division of Intramural Research, National Institute of Environmental Health Sciences, National Institutes of Health Research Triangle Park, NC 27709

[4]Department of Internal Medicine, Section of Digestive Diseases, Yale University, New Haven, CT 06520

[5]Veterans Affairs Connecticut Healthcare System, West Haven, CT 06516

Abstract

In mammals, circadian rhythms are essential for coordinating the timing of various metabolic processes. The *Clock* gene regulates diurnal plasma triglyceride fluctuation through nuclear receptor small heterodimer partner (*Shp*, Nr0b2). Given that SHP is a critical regulator of metabolism in the liver, it is unknown whether SHP is necessary to coordinate metabolism and circadian rhythms.

Methods—S*hp*$^{+/+}$ and S*hp*$^{-/-}$ mice on a C57BL/6 background (n=3–5/group) were fed a standard chow diet and water ad libitum. Serum and livers were collected at zeitgeber time (ZT) 2, 6, 10, 14, 18 and 22. In vivo and in vitro assays include: RNA-sequencing (RNA-seq), qPCR, VLDL production, adenovirus overexpression and siRNA knockdown, serum parameters, circadian locomotor activity, oil-red O staining, transient transfection, luciferase reporter assay, ChIP assay, gel-shift assay, Co-IP, Western blots.

Results—*Shp*-deficiency had a robust global impact on major liver metabolic genes. Several components of the liver clock including Pgc-1α, Npas2 and Rorα/γ were sharply induced in *Shp*$^{-/-}$ liver. At the molecular level, SHP inhibited Npas2 gene transcription and promoter activity through interaction with Rorγ to repress Rorγ transactivation and by interacting with Rev-erbα to enhance its inhibition of Rorα activity. Conversely, Npas2 controlled the circadian rhythm of Shp expression by binding rhythmically to the Shp promoter, which was enhanced by NADH, but not

*Correspondence: Tel: 801-739-4646; li.wang@uconn.edu.
[6]These authors contributed qually to this work.

AUTHOR CONTRIBUTIONS

S.L, Y.Z, H.T, and R.S performed experiments and prepared the manuscript. S.Y helped with mouse circadian behavior study. A.M.J contributed reagents. L.W. conceived and supervised the study, and wrote the manuscript.

COMPETING FINANCIAL INTERESTS

The authors declare no competing financial interests.

NADPH. Phenotypically, *Npas2*-deficiency induced severe steatosis in $Shp^{-/-}$ mice, which was attributed to the dysregulation of lipoprotein metabolism.

Conclusion—Shp and Npas2 crosstalk is essential to maintain hepatic lipid homeostasis.

Keywords

nuclear receptor; gene regulation; circadian clock; metabolism; gene knockout

The primary mammalian circadian clock is located within the suprachiasmatic nucleus (SCN) of the anterior hypothalamus and is necessary for light entrainment of the sleep–wake cycle and locomotor activity (1). The core clock system is the end result of alternating actions of specific transcriptional activators and repressors (2). The positive transcriptional regulator, brain and muscle ARNT-like protein1 (BMAL1), forms a heterodimer with circadian locomotor output cycles kaput (CLOCK), or neuronal PAS domain protein 2 (NPAS2). These dimers activate many transcripts, most notably the period (*Per1* and *Per2*) and cryptochrome (*Cry1* and *Cry2*) genes, by binding to the E-box regulatory elements on their promoters (3). The translated PER and CRY proteins then heterodimerize and repress *Clock/Bmal1* or *Npas2/Bmal1* transcription (4). Additionally, a secondary feedback loop consisting of nuclear hormone receptors adds another level of control to the transcriptional output of the primary loop (5).

Endogenous autonomous circadian clocks exist in various peripheral tissues (6). Multiple local mediators of both core clock genes and clock-controlled rhythmic transcripts respond to stimuli originating from the SCN as well as local input signals related to metabolic states (7). *Rev-erbα* was initially identified as a clock controlling and clock-regulated gene (8), which has crucial regulatory functions in hepatic metabolism (9). Retinoic acid-related orphan nuclear receptor α/γ (RORα/γ) competes with *REV-ERBα* to bind the ROR element of the *Bmal1* promoter and activate its transcription (10). RORγ directly regulates *Npas2* transcription by binding two ROREs in its proximal promoter (11) and plays an important role in glucose and lipid metabolism (12). Peroxisome proliferator-activated receptor alpha (PPARα) binds to the *Bmal1* promoter and regulates its expression, while the CLOCK/BMAL1 heterodimer in turn regulates *Pparα*, generating a positive feedback loop (13). The PPARα coactivator-1α (PGC-1α) activates the expression of *Bmal1* and *Rev-erbα* through co-activation of RORs (14), is a part of the SIRT1 histone deacetylase complex, and may directly sense the cellular metabolic state.

Although Npas2 and Clock display overlapping functions (15, 16), *Npas2*-deficient mice show particular impairment in their adaptability to food restriction (17). The circadian rhythm of *Npas2* transcription is in phase with that of *Bmal1*, strongly indicating a joint mechanism for efficient activation of target genes (18). Both NADH and NADPH enhance the DNA-binding activity of the NPAS2/BMAL1 heterodimer, suggesting that the redox state regulates molecular clock activity (19).

Small heterodimer partner (*Shp*, Nr0b2) functions as a transcriptional repressor of genes critical to hepatic metabolism (20–25). The circadian regulation of triglyceride metabolism by the *Clock* gene is mediated by *Shp* (22). However, the role of *Shp* in controlling the

rhythmicity of metabolites and liver clock machinery remains elusive. In this study, we employed transcriptomics analysis, which identified Shp as an integral component of the liver circadian network through crosstalk with Npas2, Rorα, Rorγ, Rev-erbα, and Pgc-1α.

Materials and Methods

Mice

Shp$^{+/+}$ (C57BL/6J, WT) and *Shp*$^{-/-}$ (C57BL/6J, SKO), SHP non-transgenic control (NC) and hepatocyte specific SHP transgenic (STG) mice were described previously (20, 25, 26). Mice were fed a standard rodent chow (Harlan No. 2020X) with free access to water and maintained in a 12h/12h light/dark (LD) cycle (light on 6 AM to 6 PM), temperature-controlled (23°C), and virus-free facility. Experiments on mice were performed on males at the age of 8 weeks unless stated otherwise. Hepatocyte isolation was performed as described (27). Protocols for animal use were approved by the Institutional Animal Care and Use Committee at the University of Utah.

In vivo and in vitro Studies

Serum and liver tissues were harvested at ZT2, ZT6, ZT10, ZT14, ZT18, and ZT22. A dim red light at intensity of 1 μmol/m^{2}s was used to collect tissues in dark condition (28). For *in vivo* adenoviral transduction, male mice were injected via tail vein with purified adenoviruses at 1×10^{11} virus particles per mouse. Gene expression analysis were performed 3 days or 14 days after tail vein injection. Standard methods were used for transient transfection, luciferase reporter assay, ChIP assay, gel-shift assay, Co-IP, and Western blots (27, 29). Total and 5′ capped RNA purification from mouse liver and the PCR libraries used for RNA sequencing were as previously described (30). Detailed methods for histological analysis of liver sections can be found in our previous publication (20, 27).

Statistics Analysis

All the experiments were done in triplicate and repeated at least three times. The data are presented as the mean values ± standard error of the mean (SEM). Statistical analysis was carried out using Student's *t* test for unpaired data to compare the values between the two groups; $P < .05$ was considered statistically significant.

RESULTS

Cyclic Patterns of Liver Metabolic Genes Were Drastically Altered in *Shp*$^{-/-}$ Mice

Transcriptomics (RNA-seq) and qPCR analysis of mRNA of key genes involved in cholesterol, fatty acid, bile acid, and lipid metabolism in livers of wild-type (WT) and *Shp*$^{-/-}$ mice collected over a 12:12 hr light/dark (LD) cycle showed drastic disruption of cyclic patterns (rhythmicity or amplification) in *Shp*$^{-/-}$ mice. The peak level of HMG-CoA reductase (*Hmgcr*) was increased, whereas there was a decreased amplification of mitochondrial HMG-CoA synthase2 (*Hmgcs2*) (Figure 1A). The sterol regulatory element binding protein (SREBP) family member SREBP-1c's peak expression was decreased, whereas *Srebp-2* was largely increased in *Shp*$^{-/-}$ mice. Consistent with our previous report (21, 25), cholesterol 7 alpha-hydroxylase (*Cyp7a1*) and sterol 12 alpha-hydroxylase

(*Cyp8b1*), the critical enzymes in bile acid biosynthesis, showed a shift in phase or exhibited overly increased rhythmic expression in *Shp*$^{-/-}$ mice (Figure 1B). Despite lacking obvious rhythmicity in WT mice, FGF receptor *Fgfr4* displayed a noticeable cyclic induction in *Shp*$^{-/-}$ mice similar to *Cyp8b1*.

Expression of many other lipid metabolic genes also showed distinct changes (Figure 1C). *Pparγ1* (lipid uptake) and fibroblast growth factor 21 (*Fgf21*) were drastically downregulated in *Shp*$^{-/-}$ mice, whereas acetyl-CoA carboxylase (*Acc*, provides malonyl-CoA for FA synthesis) showed a moderate decrease in expression. In contrast, the rhythmic expression of *Pparα* (FA oxidation), scavenger receptor class B member 1 (*Sr-b1*, uptake of cholesteryl ester in reverse cholesterol transport), and very low density lipoprotein receptor (*Vldlr*, cholesterol uptake) was markedly upregulated in *Shp*$^{-/-}$ mice. Fatty acid desaturase 3 (*Fads3*) with relatively unknown function also displayed substantial elevation by *Shp*-deficiency. The up- and down-regulation of selected genes (*Cyp8b1*, *Sr-b1* and *Pparγ1*) was further confirmed by RNA-seq in livers collected at ZT6 (Figure 1D).

SHP Inhibited *Npas2* Expression via Crosstalk with the RORα, γ/REV-ERBα Network

We analyzed core clock genes and nuclear receptors in the interlocking feedback loop (Figure S1). Consistent with SHP as a repressor of *Pgc-1α* in brown fat (BAT) (24), the amplification of *Pgc-1α* mRNA was highly induced in BAT of *Shp*$^{-/-}$ mice at ZT2 (Figure 2A, 1st panel). A striking increase in peak *Pgc-1α* mRNA was also observed in *Shp*$^{-/-}$ liver (2nd panel), which was decreased in Alb-*Shp*-transgenic (STG) liver (3rd panel). This was accompanied by a shift in the circadian phase of its protein expression (4th & 5th panels).

Among all the core clock genes we analyzed (not shown), *Npas2* mRNA was strongly upregulated in *Shp*$^{-/-}$ liver and downregulated in Alb-STG liver (Figure 2B, 1st & 2nd panels), as was its protein (3rd & 4th panels), suggesting a direct inhibition by SHP. Interestingly, *Rorγ* mRNA had an almost identical expression pattern as *Npas2* mRNA in *Shp*$^{-/-}$ liver, while *Rorα* mRNA expression showed a shift in phase (Figure 2C, left 4 panels). As expected, both RORγ and RORα proteins were elevated by *Shp*-deficiency (right 3 panels).

Because *Npas2* was activated by RORα and RORγ but repressed by REV-ERBα (10), we reasoned that SHP might inhibit *Npas2* transcription by binding to RORα, RORγ, or REV-ERBα. SHP interacted with RORγ and REV-ERBα but not with RORα protein (Figure 2D, left), and inhibited the activation of the *Npas2* promoter (11) by RORγ with little effect on RORα-mediated activation (right). However, co-expression of SHP with REV-ERBα further inhibited RORα activity, suggesting that SHP acts as a co-repressor of REV-ERBα. SHP overexpression also repressed the induction of *Npas2* mRNA by RORα and RORγ in Hepa-1 cells stably expressing either protein (Figure 2E). No synergistic inhibition of *Npas2* by SHP and its co-repressor EID-1 was observed. *In vivo* knockdown of *Shp* in WT liver by *shShp*-ade increased NPAS2 protein, whereas *Shp*-ade reduced NAPS2 protein in *Shp*$^{-/-}$ liver (Figure 2F). Surprisingly, despite a higher basal level of SREBP-1c precursor (p) protein, the level of cleaved SREBP-1c protein (c) was much lower in *Shp*$^{-/-}$ liver versus WT liver. SREBP-1c cleavage was largely impaired by *Shp* knockdown (*shShp*-ade) in WT

liver but was markedly enhanced by *Shp* overexpression (*Shp*-ade) in $Shp^{-/-}$ liver. These results suggest that SHP is a bona-fide transcriptional repressor of *Npas2* through crosstalk with RORα,γ and REV-ERBα (Figure S2).

NPAS2 Activated *Shp* Gene Expression in a Feedback Regulatory Loop

A recent ChIP-seq analysis (31) revealed an oscillatory recruitment of RNA pol II, NPAS2 and BMAL1 protein to the *Shp* promoter, transcription termination site (TTS) or intergenic region (Figure S3). Of note, the circadian rhythmicity of NPAS2 binding imitated the rhythmic expression of *Shp*, suggesting that NPAS2 may activate *Shp* transcription.

A canonical E-Box (CACGTG), a binding site for BMAL1, NPAS2, and CLOCK (32), was present in the *Shp* promoter, and non-canonical E-box sequences were found around NPAS2 binding peak in TTS and intergenic region (Figure 3A). We designed three probes (#1-promoter, #3-TTS, #4-intergenic) and one negative control probe (#2) for gel-shift assays using purified His-Npas2 or His-Bmal1 protein (Figure S4). NPAS2 or BMAL1 protein alone at a higher concentration (5 μg), or NPAS2 and BMAL1 heterodimer (4) at a lower concentration (1 μg) all bound to the promoter probe; the latter was dose-dependently enhanced by NADH(19) (Figure 2B) but not by NADPH (Figure S5). Unfortunately, we could not confirm NPAS2 or BMAL1 binding to *Shp* TSS and intergenic region (not shown).

We next designed ChIP assay primers (Figure S6) and validated the specificity of antibodies against RNAPII, NPAS2 and H3K4M3 (Figure S7); the latter served as an active histone modification marker (33, 34). Several surprising results were observed. RNAPII displayed a profound rhythmic binding to the *Shp* promoter of WT liver, which was blunted in $Shp^{-/-}$ liver (Figure 3C, left). The recruitment of NPAS2 appeared as a “dual-peak” oscillation in WT liver similar to *Shp* expression (Figure S3), which was enhanced in $Shp^{-/-}$ liver (middle). The binding of H3K4Me3 to the *Shp* promoter was less rhythmic in WT liver; however, its enrichment was abolished over the LD cycle in $Shp^{-/-}$ liver (right). In addition, treatment of cells with lactate to modulate intracellular NADH levels (19) enhanced *Shp* promoter reporter activity (Figure 3D), but not the activity of reporter containing TTS or intergenic region (Figure S8, bottom left). However, liver *Shp* mRNA (Figure 3E) and protein (Figure 3F) expression was only moderately decreased by si*Npas2*, suggesting that additional factors may be involved in NPAS2 mediated *Shp* activation *in vivo*. Overall, the interplay between NPAS2 and *Shp* represents a new component of NPAS2 signaling that is likely to dictate NPAS2 activity and function.

Knockdown of Npas2 in $Shp^{-/-}$ Liver Induced Steatosis by Impeding Lipoprotein Homeostasis

$Shp^{-/-}$ mice are protected against the development of fatty liver (20, 24). The strong induction of *Npas2* and *Pgc-1α* in $Shp^{-/-}$ liver prompted us to examine their potential involvement in the regulation of steatosis under *Shp*-deficient condition. Both Npas2 and Pgc-1α remained highly induced in $Shp^{-/-}$ liver at ZT2 (Figure 2B), thus ZT2 was chosen as the time point to knockdown both genes. The *siNpas2*-ade that we generated had a 30~40% efficiency in decreasing hepatic *Npas2* mRNA, whereas *siPgc-1α*-ade (35) resulted

in a 50~60% reduction of *Pgc-1α* mRNA in *Shp*$^{-/-}$ liver (Figure 4A, left and middle). The protein expression of NPAS2 and PGC-1α was similarly diminished by their respective siRNAs (right). Intriguingly, *Npas2* mRNA was highly induced by *siPgc-1α*, and *Pgc-1α* mRNA was markedly elevated by *siNpas2*. An induction of *Pgc-1α* was also observed in *Npas2*$^{-/-}$ liver (36), while PGC-1α suppressed Bmal1 expression by activating Rev-erbα (37). Thus, NPAS2 and PGC-1α exhibit mutual inhibition of mRNA expression.

siNpas2 triggered severe steatosis as revealed by oil-red O staining of neutral lipid in *Shp*$^{-/-}$ liver, which was not observed with *siPgc-1α* alone (Figure 4B). Serum AST, bilirubin, and bile acid levels were elevated in *siNpas2*:*Shp*$^{-/-}$ mice, which was somewhat exacerbated by a combinational effect of *siNpas2* and *siPgc-1α* in *siNpas2*/*siPgc-1α:Shp*$^{-/-}$ mice (Figure 4C). It was noted that serum TG levels were decreased whereas liver TG contents were increased in *siNpas2:Shp*$^{-/-}$ or *siNpas2*/*siPgc-1α:Shp*$^{-/-}$ mice, suggesting a potential disruption of lipid metabolism by *siNpas2*. On the other hand, *siPgc-1α* had little effect on TG levels.

VLDL secretion was markedly obstructed by siNpas2 in *Shp*$^{-/-}$ mice (Figure 4D, 1st panel), which correlated with reduced expression of *ApoB*, an activator of VLDL secretion (2nd panel). Apolipoprotein A-I (APOA1) is the major protein component of high density lipoprotein (HDL) in plasma, and APOC3 inhibits hepatic uptake of triglyceride-rich particles (38). Both genes were downregulated by siNpas2 (3rd & 4th panels). Unfortunately, ChIP-seq did not detect NPAS2 binding to the *ApoB* gene (31), and we could not observe NPAS2 and/or BMAL1 activation of the *ApoB* promoter (not shown). Therefore, *ApoB* is unlikely a direct NPAS2 target.

On the other hand, the mRNA levels of *Pparα* and its target *Fgf21* (39) were not affected by *siNpas2* but were induced by *siPgc-1α* (5th & 6th panels), suggesting that the PPARα-mediated increase in fatty acid oxidation may play a role in protecting *siPgc-1α:Shp*$^{-/-}$ mice from developing steatosis compared to *siNpas2:Shp*$^{-/-}$ mice. The severe steatosis caused by *siNpas2* may in turn have inhibited the expression of *Srebp-1c* and *Fasn* (7th & 8th panels) to diminish lipid synthesis. The increased *Fasn* expression by *siPgc-1α* was in agreement with its induction in *Pgc-1α*$^{-/-}$ mice (40).

Unfortunately, siNpas2 did not show desirable knockdown efficiency in WT liver (not shown), which may be due to the low basal level of Npas2 in WT relative to *Shp*$^{-/-}$ liver (Figure 2C). Overall, our results suggest a regulatory model (Figure 4E): 1) *Shp*$^{-/-}$ mice are resistant to the development of fatty liver (20, 24), which is in part associated with upregulation of Npas2, because Npas2 knockdown in *Shp*$^{-/-}$ mice reversed this phenotype; 2) WT mice are sensitive to HFD-induced fatty liver, which is associated with high Shp and low Npas2 expression.

DISCUSSION

Shp Is an Integral Component in the Liver Circadian Clock Network

The reversal of SHP-mediated inhibition of expression of *Hmgcr* (41), *Cyp7a1* (25, 42), and *Cyp8b1* (43) in *Shp*$^{-/-}$ mice is consistent with SHP's known role as a transcriptional

repressor. Although *Srebp-1c* promoter activity was inhibited by Shp (44), decreased *Srebp-1c* mRNA and increased precursor protein was observed in $Shp^{-/-}$ mice. More surprisingly, Shp overexpression enhanced SREBP-1c cleavage to generate its mature form; the latter is responsible for stimulating lipogenesis. The results suggest a potential new mechanism for post-translational regulation of SREBP-1c protein by Shp. Importantly, most of the metabolic genes analyzed exhibited an oscillatory pattern of expression, consistent with the notion that circadian rhythms and cellular metabolism are intimately linked (45). The overall gene expression profile altered by *Shp*-deficiency favors a lipid lowering phenotype, suggesting that SHP mainly serves as a modulator of metabolic homeostasis.

At the molecular level, we revealed a feedback regulatory loop between Npas2 and Shp. SHP inhibits Npas2 transcription by repressing Rorγ transactivation of the Npas2 promoter or by enhancing Rev-erbα inhibition. NPAS2 activates *Shp* gene expression by binding rhythmically to the *Shp* promoter, complementing an additional layer of control of *Shp* rhythmic expression by CLOCK (46). Overall, our findings suggest that SHP functions as an integral component of the liver circadian clock network by interfacing with RORα, RORγ, or REV-ERBα pathways to modulate the regulation and function of Npas2.

The Interplay between SHP and NPAS2 Maintains Triglyceride and Lipoprotein Homeostasis

We discovered a novel interplay between NPAS2 and SHP to maintain triglyceride and lipoprotein homeostasis (Figure S9). $Shp^{-/-}$ mice were protected against fatty liver (24) at least in part due to increased VLDL secretion (20). This phenotype was reversed by knockdown of *Npas2*, which caused severe steatosis and impaired VLDL production. Concurrently, the expression of numerous genes in lipoprotein metabolism was downregulated by siNpas2. A recent study showed that the primary dysregulated pathways in $Npas2^{-/-}$ mice uniformly converged on lipid metabolism (36). Importantly, dysregulation of NPAS2 was reported in alcohol-induced hepatic steatosis (47). Additional clinical studies also linked genomic variants of NPAS2 to the risk factors of metabolic syndrome (29). Taken together, findings from other groups and ours highlight the importance of NPAS2 in maintaining circadian rhythm mediated lipid homeostasis. Further investigation is needed to explore the role of NPAS2 in human NAFLD and AFL. It is postulated that modulating Npas2 function may open new avenues for therapeutic intervention of fatty liver disease.

In conclusion, our study reinforces the notion that SHP serves as a molecular switch that synchronizes metabolic functions to the liver circadian timing cues through a multiple regulatory modes.

Supplementary Material

Refer to Web version on PubMed Central for supplementary material.

Acknowledgments

Financial Support

L.W. is supported by NIH DK080440, AHA 13GRNT14700043, VA Merit Award 1I01BX002634, P30 DK020579 by the Diabetes Research Center at Washington University, and P30 CA042014 from Huntsman Cancer Institute. S.L. is supported by AHA Postdoctoral fellowship 13POST14630070. H.T. is supported by Manpei Suzuki Diabetes Foundation and Mochida Memorial Foundation for Medical and Pharmaceutical Research. R.S. is supported by AHA Predoctoral fellowship 14PRE17930013.

We thank the Microarray and Genomic Analysis Core for RNA-seq analysis.

References

1. Saper CB, Scammell TE, Lu J. Hypothalamic regulation of sleep and circadian rhythms. Nature. 2005; 437:1257–1263. [PubMed: 16251950]
2. Gachon F, Nagoshi E, Brown SA, Ripperger J, Schibler U. The mammalian circadian timing system: from gene expression to physiology. Chromosoma. 2004; 113:103–112. [PubMed: 15338234]
3. Rey G, Reddy AB. Connecting cellular metabolism to circadian clocks. Trends Cell Biol. 2013; 23:234–241. [PubMed: 23391694]
4. Ko CH, Takahashi JS. Molecular components of the mammalian circadian clock. Hum Mol Genet. 2006; 15(Spec No 2):R271–277. [PubMed: 16987893]
5. Duez H, Staels B. The nuclear receptors Rev-erbs and RORs integrate circadian rhythms and metabolism. Diab Vasc Dis Res. 2008; 5:82–88. [PubMed: 18537094]
6. Storch KF, Lipan O, Leykin I, Viswanathan N, Davis FC, Wong WH, Weitz CJ. Extensive and divergent circadian gene expression in liver and heart. Nature. 2002; 417:78–83. [PubMed: 11967526]
7. Yang X, Downes M, Yu RT, Bookout AL, He W, Straume M, Mangelsdorf DJ, et al. Nuclear receptor expression links the circadian clock to metabolism. Cell. 2006; 126:801–810. [PubMed: 16923398]
8. Preitner N, Damiola F, Lopez-Molina L, Zakany J, Duboule D, Albrecht U, Schibler U. The orphan nuclear receptor REV-ERBalpha controls circadian transcription within the positive limb of the mammalian circadian oscillator. Cell. 2002; 110:251–260. [PubMed: 12150932]
9. Yin L, Wu N, Curtin JC, Qatanani M, Szwergold NR, Reid RA, Waitt GM, et al. Rev-erbalpha, a heme sensor that coordinates metabolic and circadian pathways. Science. 2007; 318:1786–1789. [PubMed: 18006707]
10. Takeda Y, Jothi R, Birault V, Jetten AM. RORgamma directly regulates the circadian expression of clock genes and downstream targets in vivo. Nucleic Acids Res. 2012; 40:8519–8535. [PubMed: 22753030]
11. Takeda Y, Kang HS, Angers M, Jetten AM. Retinoic acid-related orphan receptor gamma directly regulates neuronal PAS domain protein 2 transcription in vivo. Nucleic Acids Res. 2011; 39:4769–4782. [PubMed: 21317191]
12. Burris TP, Busby SA, Griffin PR. Targeting orphan nuclear receptors for treatment of metabolic diseases and autoimmunity. Chem Biol. 2012; 19:51–59. [PubMed: 22284354]
13. Canaple L, Rambaud J, Dkhissi-Benyahya O, Rayet B, Tan NS, Michalik L, Delaunay F, et al. Reciprocal regulation of brain and muscle Arnt-like protein 1 and peroxisome proliferator-activated receptor alpha defines a novel positive feedback loop in the rodent liver circadian clock. Mol Endocrinol. 2006; 20:1715–1727. [PubMed: 16556735]
14. Liu C, Li S, Liu T, Borjigin J, Lin JD. Transcriptional coactivator PGC-1alpha integrates the mammalian clock and energy metabolism. Nature. 2007; 447:477–481. [PubMed: 17476214]
15. Reick M, Garcia JA, Dudley C, McKnight SL. NPAS2: an analog of clock operative in the mammalian forebrain. Science. 2001; 293:506–509. [PubMed: 11441147]
16. Rudic RD, Curtis AM, Cheng Y, FitzGerald G. Peripheral clocks and the regulation of cardiovascular and metabolic function. Methods Enzymol. 2005; 393:524–539. [PubMed: 15817310]
17. Dudley CA, Erbel-Sieler C, Estill SJ, Reick M, Franken P, Pitts S, McKnight SL. Altered patterns of sleep and behavioral adaptability in NPAS2-deficient mice. Science. 2003; 301:379–383. [PubMed: 12843397]

18. Yamamoto T, Nakahata Y, Soma H, Akashi M, Mamine T, Takumi T. Transcriptional oscillation of canonical clock genes in mouse peripheral tissues. BMC Mol Biol. 2004; 5:18. [PubMed: 15473909]
19. Rutter J, Reick M, Wu LC, McKnight SL. Regulation of clock and NPAS2 DNA binding by the redox state of NAD cofactors. Science. 2001; 293:510–514. [PubMed: 11441146]
20. Huang J, Iqbal J, Saha PK, Liu J, Chan L, Hussain MM, Moore DD, et al. Molecular characterization of the role of orphan receptor small heterodimer partner in development of fatty liver. Hepatology. 2007; 46:147–157. [PubMed: 17526026]
21. Zhang Y, Hagedorn CH, Wang L. Role of nuclear receptor SHP in metabolism and cancer. Biochim Biophys Acta. 2011; 1812:893–908. [PubMed: 20970497]
22. Pan X, Zhang Y, Wang L, Hussain MM. Diurnal regulation of MTP and plasma triglyceride by CLOCK is mediated by SHP. Cell Metab. 2010; 12:174–186. [PubMed: 20674862]
23. Tabbi-Anneni I, Cooksey R, Gunda V, Liu S, Mueller A, Song G, McClain DA, et al. Overexpression of nuclear receptor SHP in adipose tissues affects diet-induced obesity and adaptive thermogenesis. Am J Physiol Endocrinol Metab. 2010; 298:E961–970. [PubMed: 20124506]
24. Wang L, Liu J, Saha P, Huang J, Chan L, Spiegelman B, Moore DD. The orphan nuclear receptor SHP regulates PGC-1alpha expression and energy production in brown adipocytes. Cell Metab. 2005; 2:227–238. [PubMed: 16213225]
25. Wang L, Lee YK, Bundman D, Han Y, Thevananther S, Kim CS, Chua SS, et al. Redundant pathways for negative feedback regulation of bile acid production. Dev Cell. 2002; 2:721–731. [PubMed: 12062085]
26. Zhang Y, Xu P, Park K, Choi Y, Moore DD, Wang L. Orphan receptor small heterodimer partner suppresses tumorigenesis by modulating cyclin D1 expression and cellular proliferation. Hepatology. 2008; 48:289–298. [PubMed: 18537191]
27. Zhang Y, Soto J, Park K, Viswanath G, Kuwada S, Abel ED, Wang L. Nuclear receptor SHP, a death receptor that targets mitochondria, induces apoptosis and inhibits tumor growth. Mol Cell Biol. 2010; 30:1341–1356. [PubMed: 20065042]
28. Shi S, Hida A, McGuinness OP, Wasserman DH, Yamazaki S, Johnson CH. Circadian clock gene Bmal1 is not essential; functional replacement with its paralog, Bmal2. Curr Biol. 2010; 20:316–321. [PubMed: 20153195]
29. Englund A, Kovanen L, Saarikoski ST, Haukka J, Reunanen A, Aromaa A, Lonnqvist J, et al. NPAS2 and PER2 are linked to risk factors of the metabolic syndrome. J Circadian Rhythms. 2009; 7:5. [PubMed: 19470168]
30. Smalling RL, Delker DA, Zhang Y, Nieto N, McGuiness MS, Liu S, Friedman SL, et al. Genome-wide transcriptome analysis identifies novel gene signatures implicated in human chronic liver disease. Am J Physiol Gastrointest Liver Physiol. 305:G364–374. [PubMed: 23812039]
31. Koike N, Yoo SH, Huang HC, Kumar V, Lee C, Kim TK, Takahashi JS. Transcriptional architecture and chromatin landscape of the core circadian clock in mammals. Science. 2012; 338:349–354. [PubMed: 22936566]
32. Ripperger JA, Schibler U. Rhythmic CLOCK-BMAL1 binding to multiple E-box motifs drives circadian Dbp transcription and chromatin transitions. Nat Genet. 2006; 38:369–374. [PubMed: 16474407]
33. Bernstein BE, Kamal M, Lindblad-Toh K, Bekiranov S, Bailey DK, Huebert DJ, McMahon S, et al. Genomic maps and comparative analysis of histone modifications in human and mouse. Cell. 2005; 120:169–181. [PubMed: 15680324]
34. Heintzman ND, Stuart RK, Hon G, Fu Y, Ching CW, Hawkins RD, Barrera LO, et al. Distinct and predictive chromatin signatures of transcriptional promoters and enhancers in the human genome. Nat Genet. 2007; 39:311–318. [PubMed: 17277777]
35. Koo SH, Satoh H, Herzig S, Lee CH, Hedrick S, Kulkarni R, Evans RM, et al. PGC-1 promotes insulin resistance in liver through PPAR-alpha-dependent induction of TRB-3. Nat Med. 2004; 10:530–534. [PubMed: 15107844]

36. O'Neil D, Mendez-Figueroa H, Mistretta TA, Su C, Lane RH, Aagaard KM. Dysregulation of Npas2 leads to altered metabolic pathways in a murine knockout model. Mol Genet Metab. 2013; 110:378–387. [PubMed: 24067359]
37. Estall JL, Ruas JL, Choi CS, Laznik D, Badman M, Maratos-Flier E, Shulman GI, et al. PGC-1alpha negatively regulates hepatic FGF21 expression by modulating the heme/Rev-Erb(alpha) axis. Proc Natl Acad Sci U S A. 2009; 106:22510–22515. [PubMed: 20018698]
38. Mendivil CO, Zheng C, Furtado J, Lel J, Sacks FM. Metabolism of very-low-density lipoprotein and low-density lipoprotein containing apolipoprotein C-III and not other small apolipoproteins. Arterioscler Thromb Vasc Biol. 2010; 30:239–245. [PubMed: 19910636]
39. Inagaki T, Dutchak P, Zhao G, Ding X, Gautron L, Parameswara V, Li Y, et al. Endocrine regulation of the fasting response by PPARalpha-mediated induction of fibroblast growth factor 21. Cell Metab. 2007; 5:415–425. [PubMed: 17550777]
40. Leone TC, Lehman JJ, Finck BN, Schaeffer PJ, Wende AR, Boudina S, Courtois M, et al. PGC-1alpha deficiency causes multi-system energy metabolic derangements: muscle dysfunction, abnormal weight control and hepatic steatosis. PLoS Biol. 2005; 3:e101. [PubMed: 15760270]
41. Datta S, Wang L, Moore DD, Osborne TF. Regulation of 3-hydroxy-3-methylglutaryl coenzyme A reductase promoter by nuclear receptors liver receptor homologue-1 and small heterodimer partner: a mechanism for differential regulation of cholesterol synthesis and uptake. J Biol Chem. 2006; 281:807–812. [PubMed: 16282330]
42. Goodwin B, Jones SA, Price RR, Watson MA, McKee DD, Moore LB, Galardi C, et al. A regulatory cascade of the nuclear receptors FXR, SHP-1, and LRH-1 represses bile acid biosynthesis. Mol Cell. 2000; 6:517–526. [PubMed: 11030332]
43. Zhang M, Chiang JY. Transcriptional regulation of the human sterol 12alpha-hydroxylase gene (CYP8B1): roles of heaptocyte nuclear factor 4alpha in mediating bile acid repression. J Biol Chem. 2001; 276:41690–41699. [PubMed: 11535594]
44. Watanabe M, Houten SM, Wang L, Moschetta A, Mangelsdorf DJ, Heyman RA, Moore DD, et al. Bile acids lower triglyceride levels via a pathway involving FXR, SHP, and SREBP-1c. J Clin Invest. 2004; 113:1408–1418. [PubMed: 15146238]
45. Eckel-Mahan KL, Patel VR, de Mateo S, Orozco-Solis R, Ceglia NJ, Sahar S, Dilag-Penilla SA, et al. Reprogramming of the circadian clock by nutritional challenge. Cell. 2013; 155:1464–1478. [PubMed: 24360271]
46. Oiwa A, Kakizawa T, Miyamoto T, Yamashita K, Jiang W, Takeda T, Suzuki S, et al. Synergistic regulation of the mouse orphan nuclear receptor SHP gene promoter by CLOCK-BMAL1 and LRH-1. Biochem Biophys Res Commun. 2007; 353:895–901. [PubMed: 17204240]
47. Zhou P, Ross RA, Pywell CM, Liangpunsakul S, Duffield GE. Disturbances in the murine hepatic circadian clock in alcohol-induced hepatic steatosis. Sci Rep. 2014; 4:3725. [PubMed: 24430730]

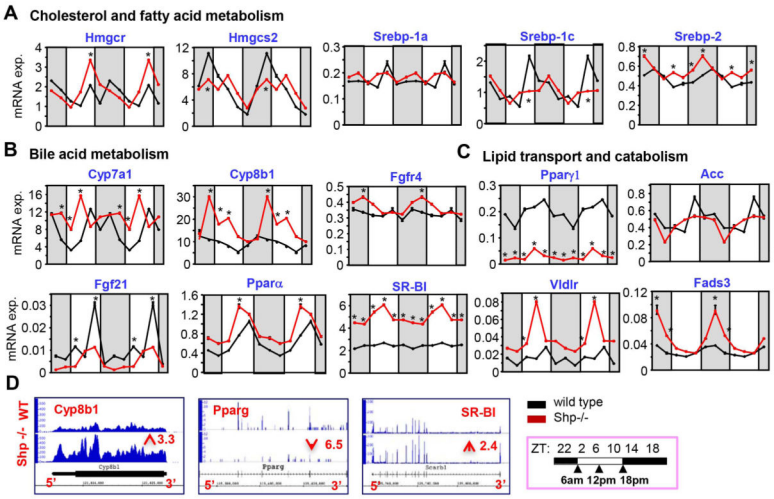

Figure 1. *Shp*-Deficiency Drastically Alters the Rhythmicity of Liver Metabolic Genes

(AC) qPCR analysis of the circadian rhythmic expression of genes involved in cholesterol and fatty acid synthesis, bile acid and lipid metabolism in wild-type and *Shp*$^{-/-}$ mice across the assayed time points. **(D)** Integrated genome browser visualization of RNA-Seq read coverage for Cyp8b1, Pparγ, and Sr-bI in wild-type and *Shp*$^{-/-}$ mice. Data are mean ± s.d. from *n*=5 mice for each time point.

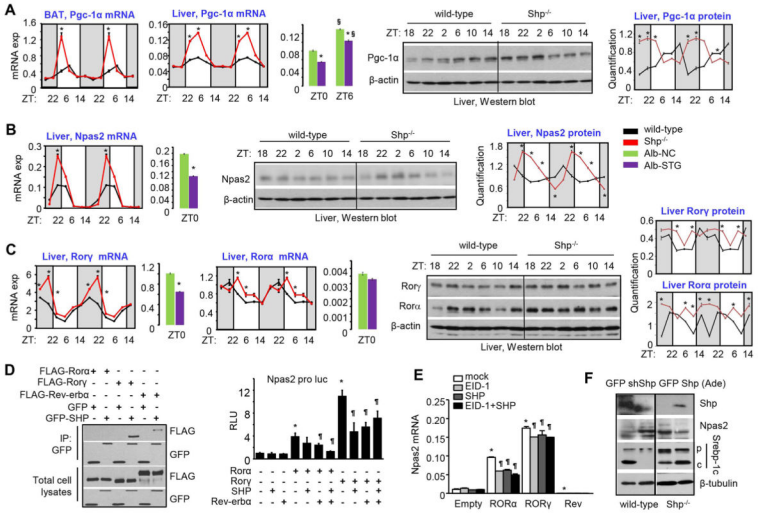

Figure 2. SHP Inhibits *Npas2* Expression via Crosstalk with the Rorα, γ/Rev-ERBα Network

(A) Left: qPCR analysis of circadian rhythmic expression of Pgc-1α in brown adipose tissue (1st panel) and liver (2nd panel) from wild-type and *Shp*$^{-/-}$ mice, and in liver of hepatocyte specific *Shp* transgenic (Alb-STG) and non-transgenic control mice (Alb-NC) (3rd panel). * $P < .01$ vs. corresponding control. § $P < .01$ vs. ZT0. Right: Western blot (4th panel) and quantitative analysis (5th panel) of Pgc-1α protein from liver extracts in wild-type and *Shp*$^{-/-}$ mice. **(B)** Left: qPCR analysis of circadian rhythmic expression of Npas2 in liver of wild-type and *Shp*$^{-/-}$ mice (1st panel) and in liver of Alb-NC and Alb-STG at ZT0 (2nd panel). * $P < .01$ vs. control. Right: Western blot (3rd panel) and quantitative analysis (4th panel) of Npas2 protein in liver of wild-type and *Shp*$^{-/-}$ mice. **(C)** Left 4: qPCR analysis of Rorα and Rorγ in in liver of wild-type and *Shp*$^{-/-}$ mice, and in liver of Alb-NC and Alb-STG at ZT0. Right 3: Western blot and quantitative analysis of Rorα and Rorγ protein in liver of wild-type and *Shp*$^{-/-}$ mice. Data are mean ± s.d. from n=5 mice for each time point. **(D)** Left: Co-immunoprecipitation (IP) followed by Western blot to determine proteins interaction of Shp with Rorα, Rorγ, or Rev-erbα. HEK293T cells were transfected with expression plasmids and cultured for 48 hr. Right: Luciferase reporter assay in HEK293T cells transfected with *Npas2*-Luc and expression plasmids for *Rorα, Rorγ, Shp* and *Rev-erbα* alone or in combination. **(E)** qPCR analysis of *Npas2* expression in stable *Rorα, Rorγ, or Rev-erbα* Hepa1-6 cells transiently transfected with *Shp* and *Eid1* alone or in combination. * $P < .01$ vs. control cell line. ¶ $P < .01$ vs. mock transfection. **(F)** Western blot of hepatic protein in WT mice subjected with *Shp* knockdown or *Shp*$^{-/-}$ mice subjected with *Shp* overexpression by adenovirus through tail vein injection.

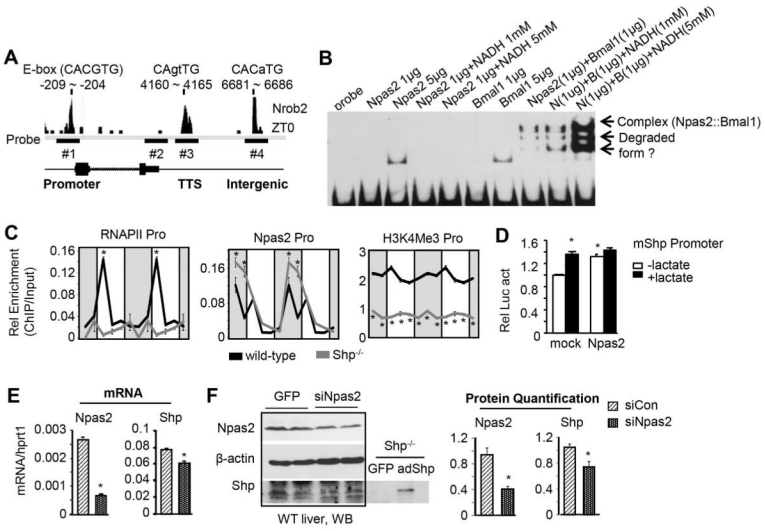

Figure 3. NPAS2 Activates *Shp* Gene Expression in a Feedback Regulatory Loop

(A) ChIP-seq signal showing binding of Npas2 to the E-box sequence (CANNTG) on *Shp* gene at ZT0 and the location of probes designed for gel-shift assay. Probe #1: the *Shp* promoter. Probe #2: 3′-untranlated region and worked as a negative control. Probe #3: transcription termination site (TTS). Probe #4: intergenic region. **(B)** NPAS2 and BMAL1 proteins were subjected to gel-shift assays with probe #1 in the presence of varying amounts of NADH. **(C)** ChIP assay and qPCR to determine the relative enrichment of RNAPII, NPAS2, and H3K4ME3 to the promoter region on *Shp* gene in the liver of wild-type and $Shp^{-/-}$ mice. **(D)** Luciferase reporter assay to determine the transactivation of Npas2 on the *Shp* promoter in the presence of lactate. **P* < .01 vs. mock control. **(E-F)** qPCR (E) and Western blot (F) of Npas2 and Shp expression in the liver of wild-type mice subjected with adenovirus siRNA targeting *Npas2* (ZT2). **P* < .01 vs. siRNA Control.

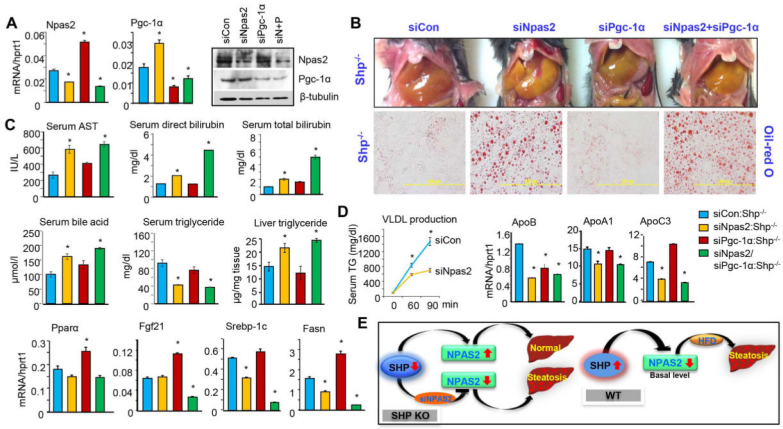

Figure 4. *Npas2*-Deficiency Sensitizes *Shp*$^{-/-}$ Mice to Steatosis

(A) qPCR and Western blot analysis of Npas2 and Pgc-1a mRNA (left) and protein (right) in liver of *Shp*$^{-/-}$ mice subjected with adenovirus siRNAs targeting *Npas2* or *Pgc-1α*, alone or in combination (ZT2). Liver tissues were harvested 4 days post adenovirus tail vein injection. Non-targeting siRNA adenovirus was included as control. Data are mean ± s.d. from *n*=5 mice for each group. * $P < .01$ vs. control. **(B)** Histological analysis of liver steatosis in *Shp*$^{-/-}$ mice subjected with adenovirus si*Npas2* and si*Pgc-1α*. Top, gross morphology of liver. Bottom, oil-red O staining of liver sections. **(C)** Serum parameter analysis and measurement of serum and liver triglyceride levels in *Shp*$^{-/-}$ mice subjected with adenovirus siRNAs. **(D)** Left: Measurement of VLDL production. Mice were subjected with adenovirus siRNAs for 7 days followed by overnight-fasting, intravenous injection with tyloxapol, and serum TG levels were examined. Right 7 panels: qPCR analysis of genes involved in lipoprotein and lipid metabolism in liver of *Shp*$^{-/-}$ mice subjected with adenovirus siRNAs. **(E)** Proposed regulatory model that elucidates a role of Npas2 in Shp-mediated steatosis.